# Development of ISUM element to represent collapse behavior of girder structure and its application to the collapse analysis of double bottom structures

*Kinya Ishibashi* *

## 1. INTRODUCTION

### 1.1 Background to the research

When a ship encounters extremely severe weather conditions, and some of its members are damaged because of collision or grounding, or if the plating thickness has reduced due to corrosion and thickness diminution and it can no longer demonstrate the initial rigidity and strength, then not only is there a chance of damage to local structural elements, but also there is a possibility of overall collapse of the structure. Such a collapse of the ship, as observed from past instances, is directly linked to loss of lives and marine pollution from oil spills, which may develop into a social problem. By introducing reliability engineering as the concept of structural safety of the ship, the probability of major accident to a ship can be evaluated. Consequently, the concept of setting levels of risks related to ship accidents that are acceptable to the society has been gaining popularity. The Common Structural Rules (CSR) of IACS evaluates the ultimate hull girder strength for hull breakage, which is the most typical mode of overall collapse of the hull, and specifies requirements to restrict such a risk to a standard level acceptable to the society.

To evaluate the probability of overall collapse of the hull, however, all scenarios that can cause hull structural damage and collapse modes need to be assumed. Loads acting on hull structures in such scenarios must be estimated with good accuracy. Moreover, progressive collapse of structural elements, such as panel and stiffened panel until the overall collapse must be represented so that the ultimate strength of the hull structure can be estimated. To respond to this requirement, using elastoplastic large deflection analysis considering geometric and material non-linearity as an evaluation tool is probably the most fundamental method of solving this problem. Fine mesh size expressing buckling and collapse of structural elements is necessary in elastoplastic large deflection analysis using the finite element method. If the structure to be evaluated is a large scale structure such as a ship structure, the number of nodes of the model and the number of degrees of freedom also become very large. However, it is very difficult to perform elasto-plastic large deflection analysis of a large scale model with a large number of degrees of freedom because of the limitations of memory capacity and processing power. Accordingly, the development of an elastoplastic large deflection analysis method with excellent calculating efficiency and high accuracy as a design tool or a strength evaluation tool for hull structure, which also considers the degradation in rigidity due to yield of buckling of the material, is anticipated.

### 1.2 About the status of research related to idealized structural unit method

The idealized structural unit method (ISUM) is an analysis method based on a new concept that enables collapse analysis for general structures, and was proposed by Rashed et al. [3),4),5)]ISUM is a method that makes use of matrix calculations similar to ordinary Finite Element Method (FEM); however, the elements used in ISUM are much larger than FEM elements. The geometric and material non-linearity are idealized and included in equations that express the rigidity of the ISUM element. Increasing the size of the element means reducing the number of nodes, which essentially means reducing the unknown number of degrees of freedom to be solved. Accordingly, the time for ISUM analysis becomes much shorter than that for FEM.

There is no change in the fundamental concept of ISUM even today. However, after the proposal by professor emeritus Ueda, revisions have been made by many researchers, and the idealization method has developed significantly. The technological development of ISUM until now can be divided into the three generations mentioned below.

The first generation ISUM element proposed initially uses a method that takes buckling of plates causing

* Research Institute

decrease in rigidity under compressive loads, as reduction in the effective width of panel, and expresses this reduction in effective width by a numerical formula. The ISUM element based on this method was developed during subsequent research to cope with combined loads expressing decrease in load-carrying capacity after ultimate strength, etc., and increased its scope of application. On the other hand, however, the equations to express element rigidity to represent these responses became extremely complex, and further development was difficult.

The second generation ISUM element proposed by Masaoka et al [6), 7)] expressed geometric non-linear response due to buckling by expressing not only in-plane deformation but also out-of-plane deformation by shape functions used in ordinary FEM. This new technique helped to shift issues in formulating ISUM from the idealization of non-linear behavior by difficult numerical expressions to selection of correct shape functions with the minimum number of degrees of freedom.

Moreover, the third generation ISUM element developed by Fujikubo, Kaeding et al [8), 9), 10), 11)] inherited the idealization method of non-linear response by second generation shape functions, made use of new shape functions, and combined various kinds of shape functions for multiple loads. The ISUM accuracy was enhanced by using these modifications. The present generation ISUM element can represent the collapse behavior of stiffened panel by combining beam column elements with ISUM elements, thereby increasing its applicability to structures.

### 1.3 Objectives of the present research

Fujikubo, Olaru, et al [12)], carried out research on collapse analysis of double bottom structures by using Timoshenko beam elements in the girder structure, as part of the study on the application of ISUM to actual structures. This study has confirmed that collapse behavior could be correctly simulated by comparing with the results of non-linear FEM analysis. On the other hand, however, ISUM estimated ultimate strength on the unsafe side, Olaru, et al, suggested that buckling due to in-plane bending loads of floors observed in non-linear FEM (hereafter called "buckling in in-plane bending") was not being represented in ISUM, as a probable cause.

Therefore, the objectives of the present research are to develop ISUM element that can represent a girder structure in which buckling in in-plane bending takes place and using the developed ISUM element in the collapse analysis of double bottom structure instead of the Timoshenko beam elements used in past research to enhance the accuracy of estimation.

## 2. Development of ISUM element to represent buckling in in-plane bending

### 2.1 Objectives

To perform collapse analysis of double bottom structure with high accuracy by ISUM, which is the objective of this research, not only ISUM element that can express the so-called flange plates of the bottom shell plating and inner bottom plating, but also ISUM element that can express a girder structure consisting of floors and girders is necessary.

Until now, the third generation ISUM element has been developed mainly for expressing the structural response of flange plates. For this reason, tensile/compressive in-plane loads in two axial directions and loads due to water pressure are assumed act on this ISUM element, and it is designed to represent collapse behavior including decrease in rigidity due to buckling. Effects on elastic deformation and yielding for shear loads and in-plane bending loads can be considered in this ISUM element. Therefore, it is suitable for conditions in which low-level shear loads and in-plane bending loads act. On the other hand, when high level shear loads or in-plane bending loads acts on a girder structure, buckling occurs because of these loads, and it may affect the in-plane rigidity. It can be considered that an ISUM element that does not have the deflection functions to cope with such buckling can not cope with this phenomenon.

According to studies by Olaru et al[12)], the ultimate strength of a rectangular panel resisting shear loads in a girder structure having dimensions and stiffener spacing used commonly in the hull structure, is practically at the yield stress level. Moreover, it has also been confirmed that a tension field is formed and almost no decrease in load-carrying capacity after ultimate strength occurs. This finding means that even if deflection shape functions for shear buckling are introduced, the estimation accuracy does not improve significantly; so such factors need not be introduced. Therefore, Research has been carried out on ISUM element that can represent buckling in in-plane bending as part of the development of ISUM element for reproducing girder structure.

## 2.2 Series calculation by non-linear FEM analysis

### 2.2.1 Details of analysis conditions

Series calculations have been performed using a model in which the aspect ratio and plating thickness of panel are varied, with the purpose of studying the collapse behavior of rectangular panel under pure in-plane bending loads.

Boundary conditions are assigned as follows: simply supported on four sides for out-of-plane displacement; condition to keep two longer sides straight as shown in Fig. 1, and two equal and opposite angles of rotation θ given to the support points A and B. Moreover, the displacement in the y direction of point B is free so that no axial force is generated even when the neutral axis is shifted for yield and buckling. MSC.Marc is used in the analysis. The initial deflection mode is taken as one half wave x one half wave, and its maximum value is taken as 10% of the plate thickness. The material characteristics are as below.

| | |
|---|---|
| Yield Stress: | $\sigma_Y$=313.6 MPa |
| Young's Modulus: | E=205.8 GPa |
| Poisson's Ratio: | ν=0.3 |
| Strain Hardening Rate: | H=0.0 |

### 2.2.2 Results of analysis and discussion

Fig. 2 shows the deformation of panel of aspect ratio 2 and plate thickness 15 mm, and Fig. 3 shows the distribution of Mises' equivalent stress, as an example of the results of analysis. When bending load acts on a rectangular panel, buckling is such that deflection develops mainly on the compression side in in-plane bending of panel. For this reason, even half-waves deflection mode along x direction is generated different from the case when in-plane compressive load acts. Observing the distribution of Mises' equivalent stress (Fig. 3(b)) when the ultimate strength of the panel is reached, the parts near the shorter edge on the compression side and tension side have yielded. When the yield area near the relevant position has increased to a certain level, the ultimate strength is reached. If the angle of rotation is further increased after the ultimate strength, deflection also increases, but no noticeable change in the deflection mode is observed. The range in which the Mises' equivalent stress becomes lowest, seen in the white band parallel to the y axis in the distribution of Mises' equivalent stress, expresses the position of the neutral axis. Observing the distribution of Mises' equivalent stress of Fig. 3(c)(d), the state of shift of the neutral axis in bending to the lower side (tension side bending of structure) can be confirmed. The shift of the neutral axis is because deflection occurs mainly in the compression side in bending of the structure and such part of the plate doesn't carry compressive loads.

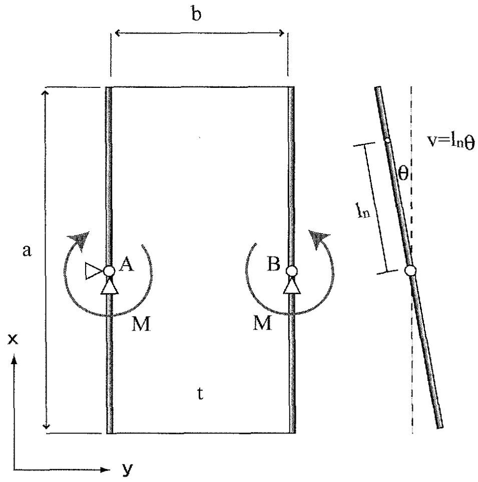


Fig. 1 Boundary and loading conditions

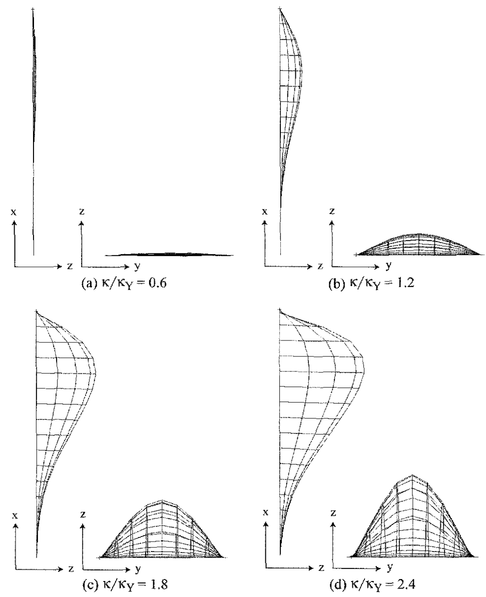


Fig. 2 Deformation of panel under in-plane bending (α2t15)

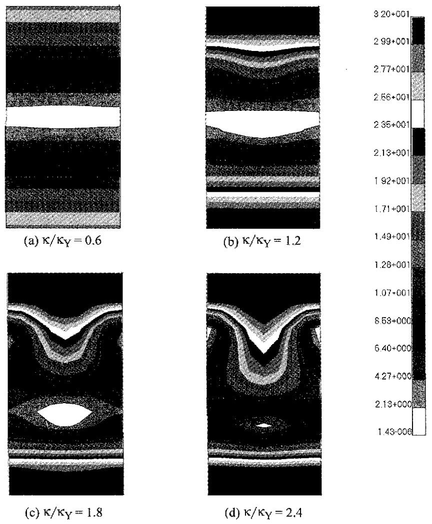

Fig. 3 Distribution of Mises' stress of bending panel

Table 1 Model for analysis

| $a/b$ / Thickness | 2.0 | 3.0 |
|---|---|---|
| 10mm | α2t10 | α3t10 |
| 15mm | α2t15 | α3t15 |
| 20mm | α2t20 | α3t20 |

Next, Fig. 4 and Fig. 5 show the relationship between angle of rotation and moment of the edges subjected to bending moments. The angle of rotation and moment are expressed as dimensionless quantities, divided by initial yield values. When the plate thickness increases, not only buckling strength and ultimate strength, but also the angle of rotation varies at the ultimate strength. The change in angle of rotation at ultimate strength according to the plating thickness means that the spread of yield area at the moment of ultimate strength varies considerably according to the plating thickness. This phenomenon is different from the collapse behavior of panel under compressive load that it surely reaches at ultimate strength when the mean compressive strain becomes almost equal to the yield strain. Moreover, the decrease in load-carrying capacity after ultimate strength is not so abrupt.

Next, the transition of out-of-plane deflection mode of panel with aspect ratio 2 and plating thickness of 15 mm of Fig. 6 is studied. A1, A2, A3, A4 express the amplitudes of one half-wave to four half-wave modes along the longer sides of the panel. From this figure, the development of one half-wave mode and two half-wave mode can be confirmed to be notable. These two modes form typical shapes for buckling in in-plane bending as shown in Fig. 2. The amplitude of deflection mode above three half-wave mode also becomes large, but the timing at which development starts is after the ultimate strength, and mainly expresses the change in deflection shape due to yield. Even in panels in which the plating thickness and aspect ratio are different, there is very little difference compared to the transition of out-of-plane deflection mode mentioned above. Incidentally, an ISUM element that has appropriate deflection function can expresses the deflection shape that occurs due to buckling more accurately and can represent the collapse behavior including change in the in-plane rigidity after buckling and ultimate strength. Consequently, based on results of studies of deflection mode obtained from non-linear FEM analysis, two proposals can be considered, one is assigning up to the two half-wave modes of A1 and A2 as deflection shape function, and the other is assigning up to the four half-wave modes of A1 to A4. To decide which of the proposals to use, trial calculations of the ISUM analysis have been carried out using both proposals in practice, considering estimation accuracy and calculation costs.

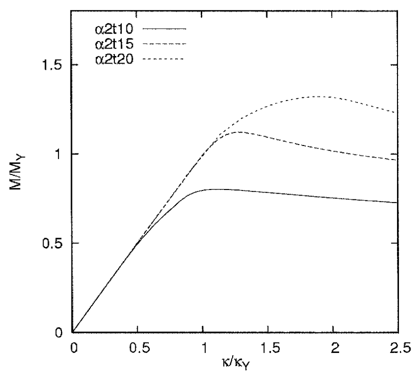

Fig. 4 Moment-curvature relationship
(aspect ratio = 2.0)

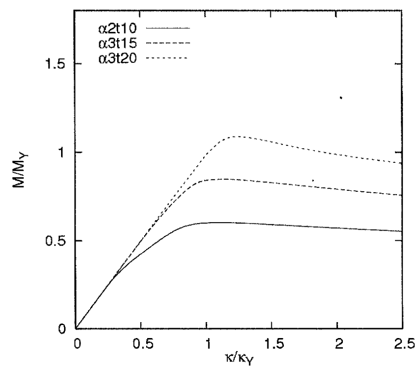

Fig. 5 Moment-curvature relationship
(aspect ratio = 3.0)

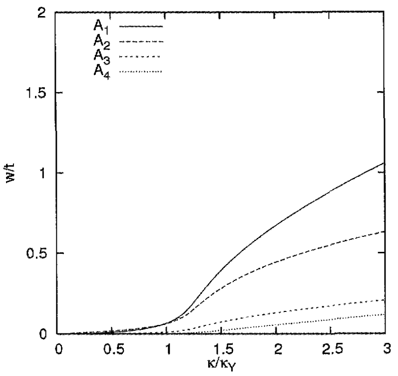


Fig. 6 Transition of deflection mode of α2t15

## 2.3 Deflection function to express buckling in in-plane bending

ISUM expresses deflection arising from buckling by a deflection function. The parameters expressing the magnitude of deflection are treated as independent degrees of freedom similar to nodal displacement The deflection functions considered in ISUM element in the past were only symmetric components such as one half-wave, three half-waves, and so on. In contrast, the deflection shape under in-plane bending load includes asymmetric components such as two half-waves and four half-waves. Accordingly, a larger number of deflection modes needs to be considered in deflection functions. For this reason, the equation below gives the general notation for a shape having multiple deflection modes.

$$w(x,y) = \sum_i^n A_i \sin\frac{i\pi}{a}x \sin\frac{\pi}{b}y \tag{1}$$

The assumption is that the initial deflection $w_0$ of the waveform same as that of equation 3.1 occurs in this panel.

$$w_0(x,y) = \sum_i^n A_{0i} \sin\frac{i\pi}{a}x \sin\frac{\pi}{b}y \tag{2}$$

By substituting equations (1) and (2) in the Airy's stress function considering large deflection, the in-plane strain-deflection relationship below can be obtained.

$$\begin{aligned}\epsilon_x =\ & \frac{\partial u}{\partial x} - \pi^2\alpha^2 \sum_i\sum_j (A_iA_j - A_{0i}A_{0j}) \\ & \times\left[\left\{\left(\frac{j(i-j)}{a^2(4+\alpha^2(i+j)^2)^2} - \frac{\nu j(i-j)(i+j)^2}{4b^2(4+\alpha^2(i+j)^2)^2}\right)\cos\frac{(i+j)\pi x}{a}\right.\right. \\ & \left.\left(\frac{j(i+j)}{a^2(4+\alpha^2(i-j)^2)^2} - \frac{\nu j(i+j)(i-j)^2}{4b^2(4+\alpha^2(i-j)^2)^2}\right)\cos\frac{(i-j)\pi x}{a}\right\}\cos\frac{2\pi y}{b} \\ & \left.-\frac{\nu}{4b^2}\left\{\frac{j}{\alpha^4(i+j)}\cos\frac{(i+j)\pi x}{a} + \frac{j}{\alpha^4(i-j)}\cos\frac{(i-j)\pi x}{a}\right\}\right] \\ & +\frac{\pi^2}{8b^2}\sum_i i^2(A_i^2 - A_{0i}^2)\end{aligned} \tag{3}$$

$$\begin{aligned}\epsilon_y =\ & \frac{\partial v}{\partial y} - \pi^2\alpha^2 \sum_i\sum_j (A_iA_j - A_{0i}A_{0j}) \\ & \times\left[\left\{\left(\frac{j(i-j)(i+j)^2}{4b^2(4+\alpha^2(i+j)^2)^2} - \frac{\nu j(i-j)}{a^2(4+\alpha^2(i+j)^2)^2}\right)\cos\frac{(i+j)\pi x}{a}\right.\right. \\ & \left.\left(\frac{j(i+j)(i-j)^2}{4b^2(4+\alpha^2(i-j)^2)^2} - \frac{\nu j(i+j)}{a^2(4+\alpha^2(i-j)^2)^2}\right)\cos\frac{(i-j)\pi x}{a}\right\}\cos\frac{2\pi y}{b} \\ & \left.+\frac{1}{4b^2}\left\{\frac{j}{\alpha^4(i+j)}\cos\frac{(i+j)\pi x}{a} + \frac{j}{\alpha^4(i-j)}\cos\frac{(i-j)\pi x}{a}\right\}\right] \\ & +\frac{\pi^2}{8a^2}\sum_i i^2(A_i^2 - A_{0i}^2)\end{aligned} \tag{4}$$

$$\begin{aligned}\gamma_{xy} =\ & \frac{\partial v}{\partial x} + \frac{\partial u}{\partial y} - \frac{(1+\nu)\alpha^2\pi^2}{ab}\sum_i\sum_j (A_iA_j - A_{0i}A_{0j}) \\ & \times\left[\frac{j(i^2-j^2)}{(4+\alpha^2(i+j)^2)^2}\sin\frac{(i+j)\pi x}{a} + \left\{\frac{j(i^2-j^2)}{(4+\alpha^2(i-j)^2)^2}\sin\frac{(i-j)\pi x}{a}\right\}\sin\frac{2\pi y}{b}\right]\end{aligned} \tag{5}$$

Since the superimposition of many deflection modes is expressed by a general notation and used to formulate a stiffness equation, the number of deflection modes and types considered can be arbitrarily changed by simple program modification.

## 2.4 Validating the accuracy of the developed ISUM element

ISUM analysis has been performed with the same analysis conditions as shown in Section 2.2, using the ISUM element having the deflection function shown in Section 2.3. 7 x 21 stiffness integration points are set in the ISUM element. Yield is judged by the Egger yield function at each integration point. Fig. 7 and Fig. 8 show the comparison of the angle of rotation-moment relationship obtained in ISUM analysis and FEM analysis using deflection functions considering two half-waves and four half-waves respectively. When modes up to two half-waves are considered, and if the aspect ratio is especially large and the plate thickness is small, then the error compared to FEM is notable. On the other hand, when modes up to four half-waves are considered, and the difference in plate thickness has been improved significantly, there is good coincidence with the results of FEM analysis up to the ultimate strength.

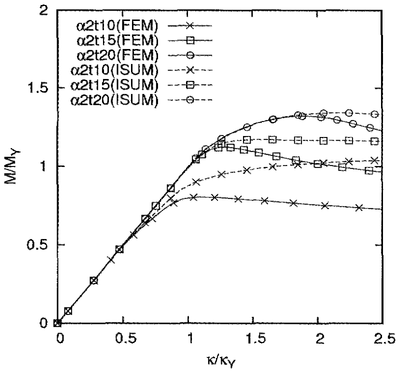


(a) Aspect ratio = 2.0

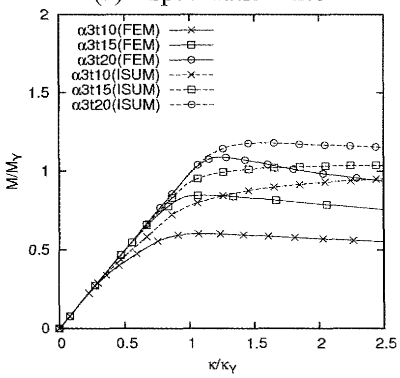


(b) Aspect ratio = 3.0

Fig. 7 Bending moment – curvature relationship considering 1 and 2 half waves modes

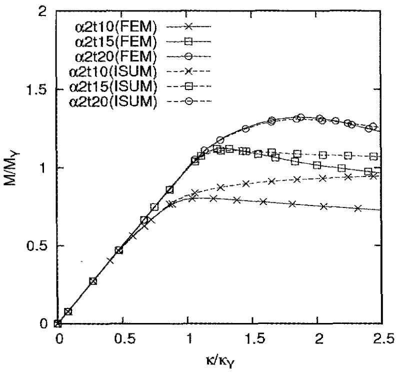


(a) Aspect ratio = 2.0

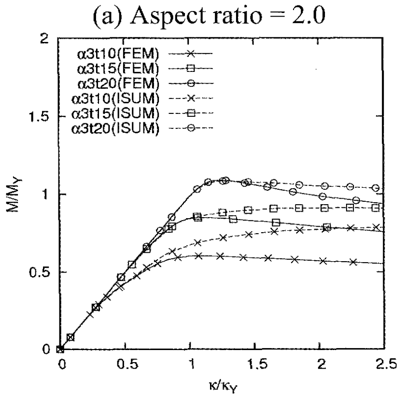


(b) Aspect ratio = 3.0

Fig. 8 Bending moment – curvature relationships considering 1 to 4 half waves modes

Next, Fig. 9 shows the comparison of amplitudes of each deflection mode for ISUM and FEM considering modes up to four half-waves. Good coincidence is found for $A_1$ to $A_3$, and the deflection shape functions shown in equation (1) are performed correctly, as predicted. However, there is a trend of estimating lower amplitude than that obtained from FEM when the angle of rotation has become large. Behaviors of A4 don't coincide between ISUM and FEM. The cause is considered to be in the estimation of in-plane strain-deflection relationship assuming elastic response of the material because $A_4$ always increases after the ultimate strength. ISUM analysis considering modes above five half-waves has been also carried out, but improvement in accuracy is not significant. A large number of deflection modes results in an increase in the number of degrees of freedom, and the original advantages of ISUM is lost. Therefore, modes up to four half-waves are considered appropriate for ISUM element expressing buckling in in-plane bending.

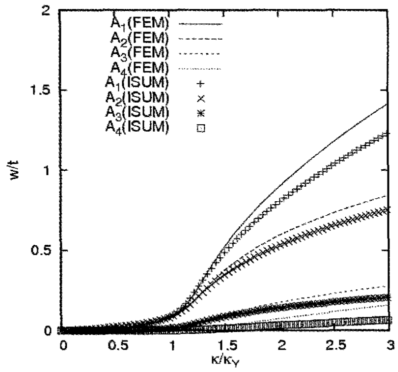


Fig. 9 Comparison on amplitudes of deflection modes (α2t15)

# 3. Collapse analysis of double bottom structure by the idealized structural unit method

## 3.1 Objectives

In this section, the collapse analysis of double bottom structure used in the girder structure of the ISUM element shown in Section 2 is performed. The first objective of the present research is to validate whether the collapse behavior and the ultimate strength of double bottom structures can be estimated by considering buckling in in-plane bending.

The collapse analysis of a double bottom structure is performed by non-linear FEM in this section to validate the collapse analysis by ISUM. Another objective of the research is to gain knowledge related to collapse behavior of double bottom structures referring to these results, in addition to the analysis results of ISUM.

## 3.2 Analysis conditions

### 3.2.1 Details of double bottom structure to be analyzed

Details of the double bottom structure of Panamax size bulk carrier (models P1 and P2) used in the analysis in this section are described here.

The dimensions and the structural arrangements are assigned based on the double bottom structure of a Panamax size bulk carrier. However, openings in the girder are not modeled. Table 2 shows the principal dimensions of this model. Fig. 10 shows the arrangement of girders and stiffeners. Horizontal stiffeners attached to girders are taken as 160 x 15 mm flat bars.

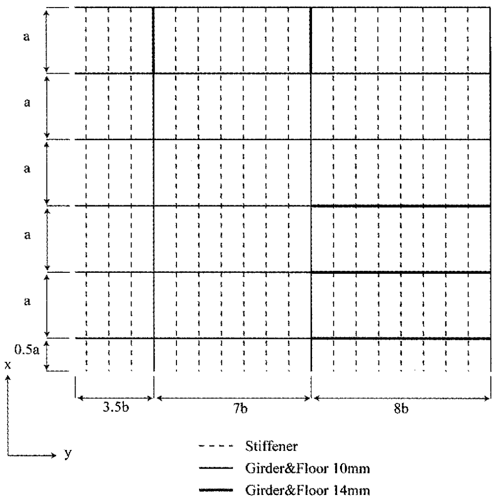


Fig. 10 Arrangements of girders and stiffeners of models P1 & P2

Table 2 Principal dimensions of double bottom structure

| Length × width ($m$) | Height ($m$) | number of floors | number of girders |
|---|---|---|---|
| 28.0×28.0 | 1.867 | 12 | 6 |
| Inner bottom thickness ($mm$) | Bottom thickness ($mm$) | Floor space a ($mm$) | Long. Space b ($mm$) |
| 18 | 15 | 2,545 | 757 |
| Girders & Floors Thickness ($mm$) | | Scantling of Inner bottom and bottom stiffeners ($mm$) | |
| Model 1 10,14 | Model 2 20, 28 | 250x90x9/15 | |
| Torsional stiffness of bilge hopper GJ (N mm$^2$) | | | |
| 6.45 x10$^{16}$ | | | |

Model P1 is prepared using dimensions close to the actual design with plating thickness at the center taken as 10 mm and at the ends as 14 mm in the girder web. Model P2 is prepared by taking twice the plating thickness of girder web derived from this model.

### 3.2.2 Boundary conditions

The boundary conditions assigned are symmetric conditions at the center in the x and y directions of the double bottom structure since the mode is one-forth region. The mid-points in the depth direction of the end sections of girders and floors are supported in the vertical direction, as shown in Fig. 11. For these support points of girders or floors, only uniform displacements occur normal to their section. As shown in Fig. 12, the end sections of girders and floors are kept straight, and they rotate about the support points. The lines joining the ends of bottom shell plating and inner bottom plating between adjacent girders and floors are kept straight. The section adjacent to the stool is simply supported as shown in Fig. 13. Torsional stiffness elements are added along the neutral axis of the section adjacent to the bilge part, and torsional stiffness is assigned assuming the bilge hopper tank. Torsional stiffness is calculated using the dimensions of bilge hopper tank of the assumed bulk carrier. The inner bottom plating is not shown in Fig. 11 to Fig. 13.

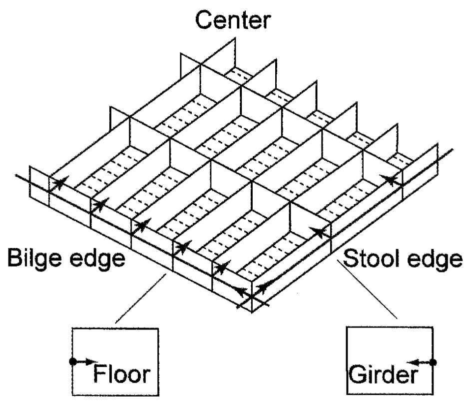


Fig. 11 Boundary conditions (axis of rotation at bottom edges)

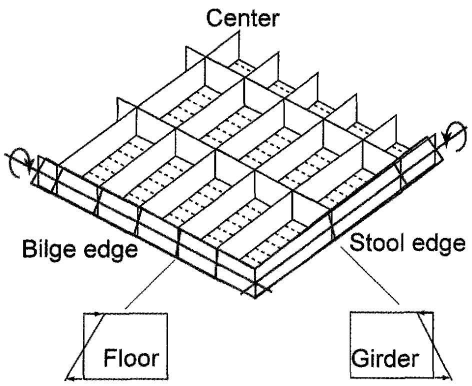


Fig. 12 Boundary conditions
(end section of floor, girder and bottom panel)

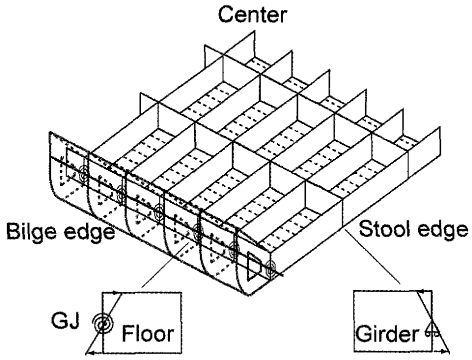


Fig. 13 Boundary condition
(rotational constraint at bilge edges)

### 3.2.3 Details of ISUM model

Details of ISUM model used for collapse analysis are described below. The stiffened panel model [9] combining ISUM element and beam-column elements proposed in the third generation ISUM is used for stiffened panels of bottom shell plating and inner bottom plating. Meshing of elements is as shown in Fig. 14, with 4 meshes between floors and one mesh between longitudinal stiffeners. The deflection shape function considered are of two types: the three half-wave mode *Al* between floors equivalent to the buckling mode for compressive loads in the direction of the longer side shown in Fig. 15, and the deflection shape *At* in cylindrical shape equivalent to the collapse mode for compressive loads in the direction of the shorter side. To satisfy continuity of deflection shape, the amplitudes of deflection shape function of the four ISUM elements between floors *Al*, *At* are each assigned the same unknown variable.

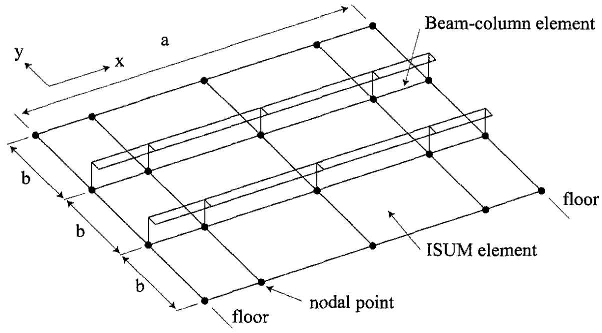


Fig. 14 ISUM / beam-column mesh for outer and inner bottom plates

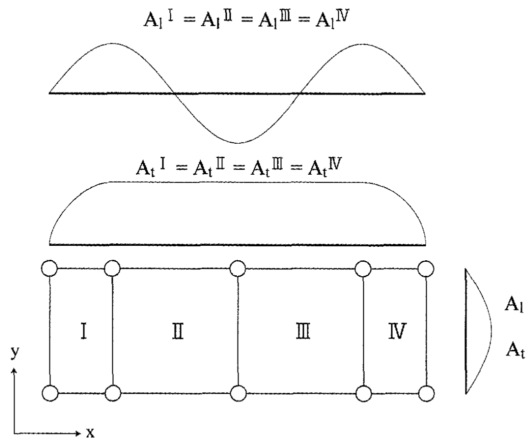


Fig. 15 Idealized deflections of outer and inner bottom plates

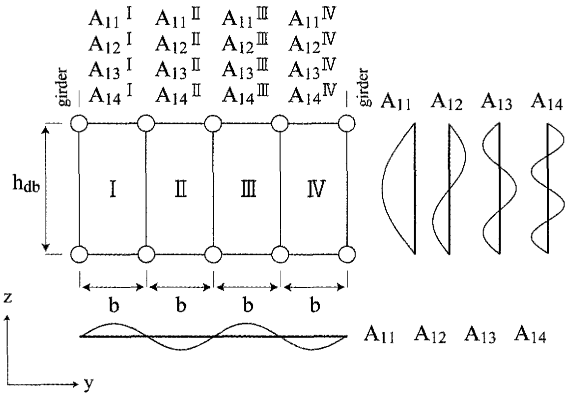


Fig. 16 Meshing and idealized deflections of floors

The ISUM element for representing buckling in in-plane bending developed in Section 2 is used for floors (Fig. 16). One mesh each is used for longitudinal space and girder depth. The deflection shape function consists of four kinds of modes from one to four half-waves in the depth direction of the girder. Independent unknown variables are assigned to the amplitude of deflection shape of individual ISUM elements. Vertical stiffeners attached to the floor are not simulated in this model. By setting the mesh size mentioned above and the deflection shape function, however, out-of-plane deformation of floor along the vertical stiffener does not occur and the effect of the vertical stiffener is considered. However, it can not consider the situation that vertical stiffeners collapse.

For girder also, the ISUM element developed in Section 2 is used. For meshing in the longitudinal direction, as shown in Fig. 17, four meshes are set to match the nodes of the elements forming the bottom shell plating and inner bottom plating, and one mesh is set in the depth direction of the girder. To consider the effects of out-of-plane deformation constraints of girder due to stiffeners in the horizontal direction attached to the girder, Only three half-wave modes in the depth direction of the girder is considered as the deflection function. Common unknown variables are assigned to the amplitude of deflection shape function of the four ISUM elements between floors.

To realize the boundary conditions shown in Section 3.2.2, nodes are assigned at the mid-position of nodal points located in the inner bottom plating and bottom shell plating (center of girder in the depth direction) at the ends of model touching the bilge hopper tank and lower stool. The displacements in z-direction of the assigned nodes are constrained. Multiple point constraining conditions are appropriately assigned to other nodes located at the ends of the model.

### 3.2.4 Details of modeling in non-linear FEM analysis

A double bottom structure is modeled using only shell elements in the collapse analysis with non-linear FEM. Meshes are given as shown in Fig. 18 and Table 3 so that buckling of local panel can be adequately represented. To reduce the calculation costs, the vertical stiffeners are not modeled by shell elements. Instead of it, constraining conditions are assigned for out-of-plane deformation of floor using multiple point constraints (RBE2). Similar to the ISUM model, multiple point constraining conditions are appropriately assigned to the nodes located at the end of the double bottom structure to realize the boundary conditions shown in Sec. 3.2.2.

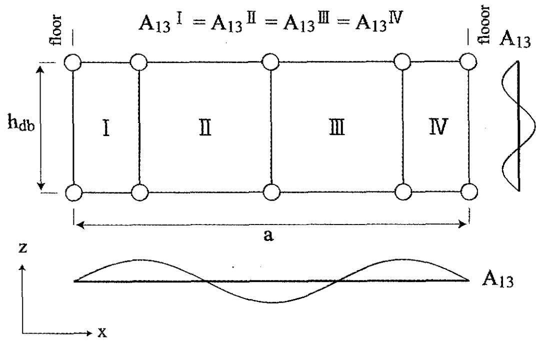


Fig. 17 Meshing and idealized deflections of girders

Table 3 Meshing and number of elements

| | FEM | ISUM |
|---|---|---|
| Between long. Stiffeners | 6 meshes | 1 mesh |
| Between trans. girders | 18 meshes | 4 meshes |
| Floor depth | 13 meshes | 1 mesh |
| Stiffener web depth | 3 meshes | 1 mesh |
| Number of Elements | 47,570 | 1,720 |

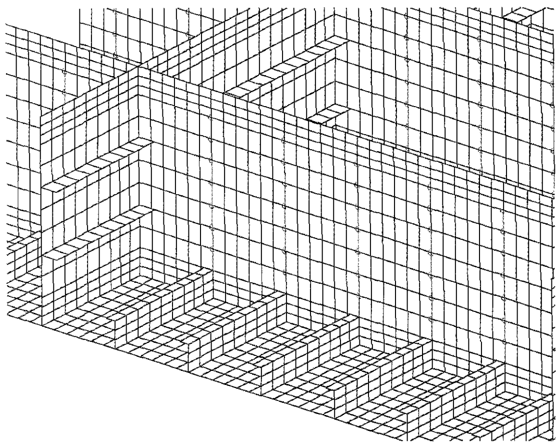

Fig. 18 Meshing for collapse analysis on double bottom structures with non-linear FEM

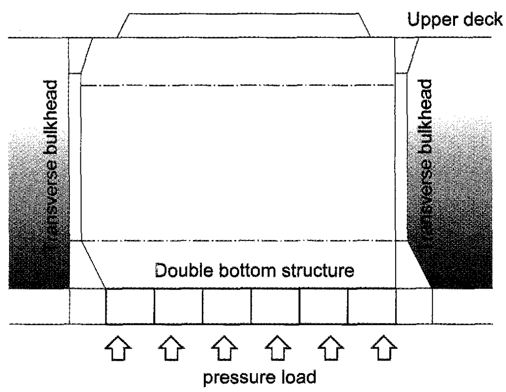


Fig. 19 Loading condition of vertical pressure load

### 3.3 Collapse analysis of double bottom structure subjected to pressure load in the vertical direction

#### 3.3.1 Loading condition

Loading condition is as shown in Fig. 19. A uniform upward pressure load acts on the bottom shell plating assuming the condition that sea water pressure acts on the bottom shell plating of the double bottom structure of an empty hold.

#### 3.3.2 Panamax size bulk carrier (Model P1)

Collapse analyses by ISUM and non-linear FEM have been carried out for double bottom structure of Panamax size bulk carrier (model P1). The results from both analyses have been compared and the accuracy of ISUM analysis has been validated. The comparison of deformation diagrams, water head-central deflection relationships, and stress distributions is described below.

The analysis is performed using the Newton-Raphson and load control scheme, so collapse behavior cannot be tracked after the condition of decrease in load-carrying capacity. However, both ISUM and FEM analyses can be performed until the rigidity reduce adequately, and the substantial maximum load carrying capacity of the structure can be obtained. The analysis time for FEM is about 6 hours and for ISUM is about 10 minutes. ISUM is demonstrated as an analysis method with adequately high efficiency.

**(a) Comparison on deformation diagrams**

Fig. 20 to Fig. 23 show the deformation diagrams obtained by non-linear FEM and ISUM analyses at a water head of 15 m and 18 m at which the ultimate strength of the structure is reached. These deformation diagrams are plotted so that the top and bottom of the double bottom structure are reversed and the bottom shell plating is shown at the top.

Firstly, observing the deformation diagrams (Fig. 20 and Fig. 21) at water head of 15 m from the results of analyses by both non-linear FEM and ISUM, buckling of the bottom shell plating occur near the central part of the double bottom subjected to compression resulted from overall bending of the double bottom structure. Moreover, buckling in in-plane bending occur near the center of the floor span (hull center line). These observations verify that the ISUM element for representing buckling in in-plane bending developed in Section 2 function correctly. On the other hand, the results of non-linear FEM show deflection in the fixed mode due to water pressure near the stool end of the bottom shell plating, but the deflection in the fixed mode from local load due to water pressure on panel could not be represented by ISUM used here. For this reason, the deflection in the ISUM results is deflection in the support mode.

At the water head of 18 m (Fig. 22 and Fig. 23) at which the double bottom structure reaches its ultimate strength, results of both analyses show that large shear deformation occurred due to yield at the girder ends. Shear deformation due to yielding and buckling in in-plane bending occur at the floor ends. Moreover, very large deflection occur in the panel near the hull center line of the bottom shell plating, indicating that the stage after the ultimate strength has been reached. The cause of buckling in in-plane bending at the floor ends is the effect of elastic torsional stiffness element considering rigidity of the bilge hopper.

As indicated above, the position and timing of occurrence of buckling and yield of structural elements obtained from the ISUM collapse analysis are verified to agree very well with the results of non-linear FEM.

**(b) Comparison of water head-central deflection relationships**

The results of analysis by ISUM and non-linear FEM related to the relationships between water head and displacement in the vertical direction at the center of the double bottom are compared, and shown in Fig. 24. Three cases of analysis by ISUM are carried out as shown in Table 4. The ISUM Case 1 in which all ISUM elements are assumed to deflect out-of-plane, showed practically the same displacement at various load levels compared to that of non-linear FEM; moreover, the ultimate strength values also coincided extremely well. For ISUM Case 2, some difference in the displacement start occurring from a water head around 5 m compared to the analysis results of non-linear FEM and ISUM Case 1. This is attributed to the decrease in the overall bending rigidity of the double bottom structure due to buckling of the bottom shell plating that occurs at a comparatively early stage, which is not represented in ISUM Case 2 since it does not allow full buckling to occur. With regard to ISUM Case 3, although the occurrence of local buckling of the bottom shell plating can be represented, the decrease in rigidity due to buckling in in-plane bending of floors observed in Fig. 20 and Fig. 21 cannot be considered. For this reason, obviously the difference arises from a water head of about 13 m compared to ISUM Case 1 and the results of non-linear FEM analysis.

In this way, since buckling cannot be represented in all or some of the members in ISUM Case 2 and Case 3, the decrease in rigidity due to buckling cannot be represented, and difference in displacement arises with the analysis results of non-linear FEM. With regard to ultimate strength, however, practically identical results are obtained. The reasons for this are described later.

Table 4 Conditions of ISUM analysis

| | |
|---|---|
| Case 1 | Normal ISUM analysis (free out-of-plane deflection of plate element) |
| Case 2 | Out-of-plane deflections of all ISUM plate elements are constrained |
| Case 3 | Out-of-plane deflections of all ISUM plate elements expressing girder are constrained |

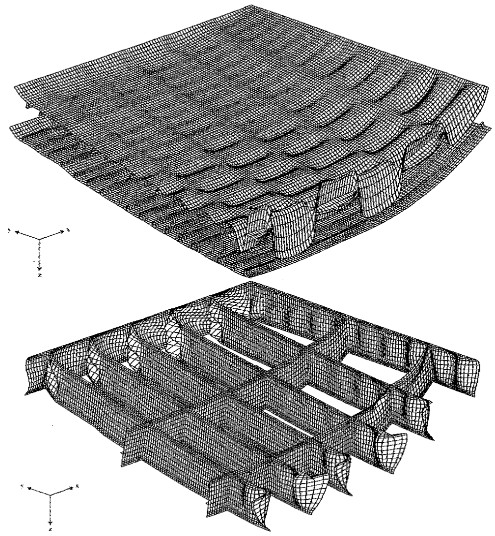

Fig. 22 Deformation at water head 18 m obtained from non-linear FEM (model P1)

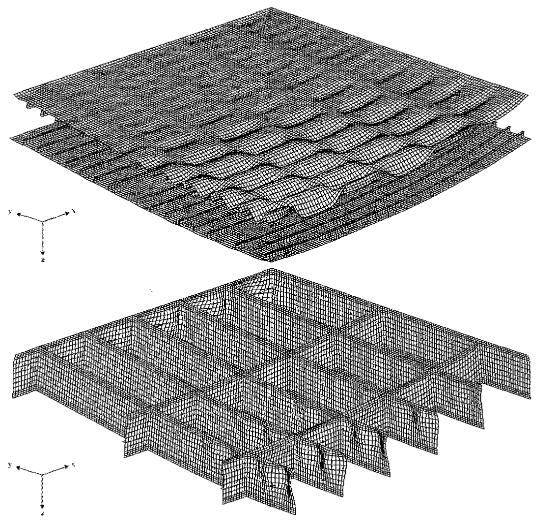

Fig. 20 Deformation at water head 15 m obtained from non-linear FEM (model P1)

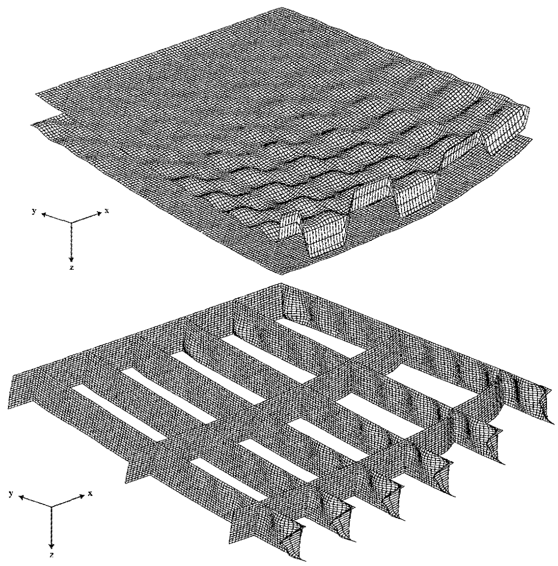

Fig. 23 Deformation at water head 18 m obtained from ISUM (model P1)

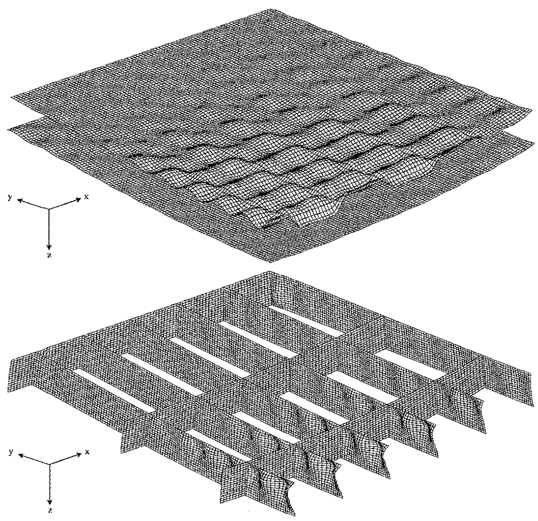

Fig. 21 Deformation at water head 15 m obtained from ISUM (model P1)

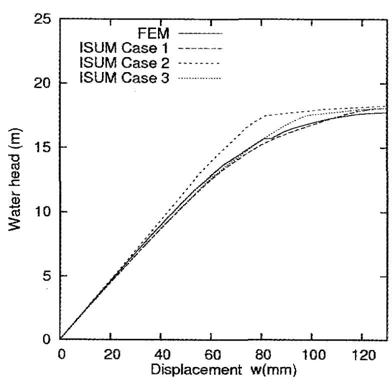


Fig. 24 Water head-central displacement relationship (model P1)

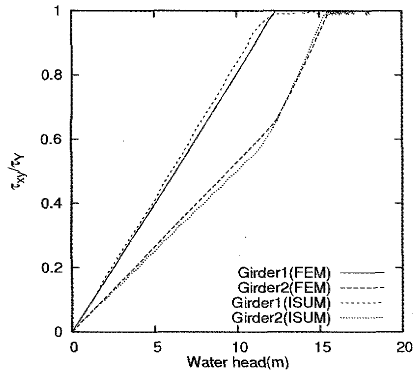


Fig. 25 Average shear stress at girder ends (model P1)

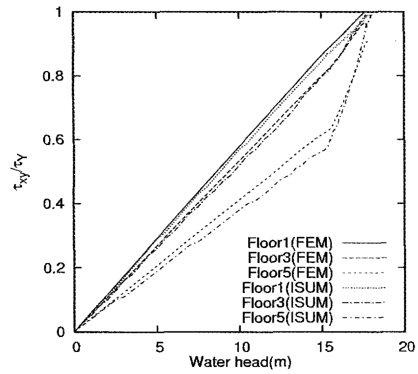


Fig. 26 Average shear stress at floor ends (model P1)

### (c) Comparison of average shear stress-water head relationships at girder ends

Fig. 25 and Fig. 26 are plots of average shear stress at the ends of girders and floors obtained from ISUM and non-linear FEM results, taking water head along the horizontal axis. As shown in Fig. 25, load redistribution occurs when Girder 1 yields. A non-linear response of the average shear stress in Girder 2 and Floor 5 is indicated, in which the rate of change increases with the water head. Moreover, shear yield occurs first in Girder 1 and then in Girder 2. All of the floors and the girders yield in shear simultaneously at the water head of 18 m, which is the instant the structure reaches ultimate strength. In view of the above, it can be concluded that the collapse of the entire structure occur at the instant all of the girders and the floors yield in shear. Even in ISUM Case 2 and ISUM Case 3 wherein buckling in panel elements is disregarded partially and entirely, almost the same ultimate strength is determined. This is because the collapse factors of double bottom structure can be considered because of the yield in shear of the girder webs and not because of panel buckling of girder webs or bottom shell plating.

### 3.3.3 Double bottom structure of Panamax size bulk carrier with increased girder dimensions (model Panel)

The overall collapse of model P1 is because of shear yield of the ends of all girders. Therefore, to study collapse factors other than shear yield of girder ends, a derived model (model P2) taking twice the web plating thickness of girder is prepared. Collapse analyses by ISUM and non-linear FEM are performed and this derived model is compared and validated.

### (a) Comparison of deformation diagrams

The deformation diagrams at ultimate strength obtained from ISUM and non-linear FEM analyses are shown in Fig. 27 to Fig. 30. Noticeable out-of-plane deformation showing collapse of floor panel at the center of floor span and collapse of bottom shell plating at the center of the double bottom, large shear deformation due to yield in the joining parts of girder ends and Girder 1 and Floor 5, buckling of the inner bottom plating at the floor ends, and buckling in in-plane bending of floor panels, etc., can be observed from the results of both analyses. Moreover, the noticeable overall bending deformation of the double bottom structure in the direction of the floors accompanying these collapses also coincides, as seen in the results of both analyses. By increasing the plating thickness of the girder web, collapse behavior evidently different from that of model P1 appears.

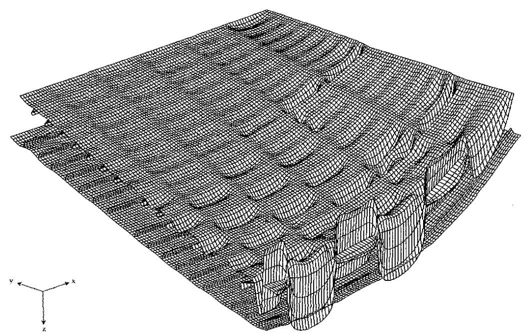

Fig. 27 Deformation of flange plates at water head 30 m obtained from non-linear FEM (model P2)

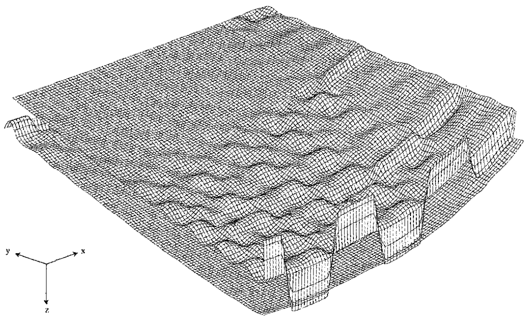

Fig. 28 Deformation of flange plates at water head 30 m obtained from ISUM (model P2)

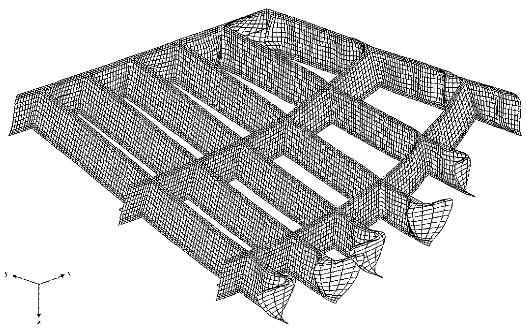

Fig. 29 Deformation of girders at water head 30 m obtained from non-linear FEM (model P2)

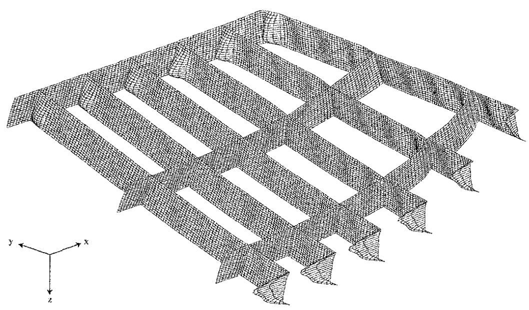

Fig. 30 Deformation of girders at water head 30 m obtained from ISUM (model P2)

### (b) Comparison of water head-central deflection relationships

Fig. 31 shows the comparison of water head-central deflection relationships obtained by ISUM and non-linear FEM analyses for model P2. Here also, analysis results for 3 cases of Table 4 are examined. Firstly, similar to model P1, the water head-deflection relationships at various water head levels for ISUM Case 1 agree very well with the results of non-linear FEM analysis, and fairly accurate ultimate strength results have also been obtained. For ISUM Case 2 and Case 3, the deflection at the intermediate loading stage and the ultimate strength differ considerably from the results of non-linear FEM analysis. In the estimation of ultimate strength of Case 2 in which the amplitude of deflection shape function of all the ISUM elements is constrained, difference occurs compared to non-linear FEM. This indicates that the local buckling of bottom shell plating and inner bottom plating panels and girder webs has affected the ultimate strength of the double bottom structure. This means that the collapse factors are different from the shear yield at girder ends, which is the collapse factor for model P1. On the other hand, even for Case 3 in which the amplitude of deflection of only ISUM element expressing girder structure is constrained, difference occurs compared to the ultimate strength of non-linear FEM. This difference is because the buckling in in-plane bending of floor in ISUM Case 3 has not been represented. Since the analysis results of ISUM Case 1 shows very good correlation with the analysis results of non-linear FEM, it can be confirmed that the buckling of floor has affected the ultimate strength, and that the ISUM element reproducing buckling in in-plane bending developed in Section 3 has functioned correctly.

### (c) Comparison of average shear stress-water head relationships at girder ends

Fig. 32 and Fig. 33 are plots showing the state of change in the average shear stress at the ends of girders and floors obtained from ISUM and non-linear FEM results with the increase in the water head. Here too, the results of ISUM analysis show excellent agreement with the results of non-linear FEM analysis. At the ultimate strength, while the girder ends have yielded in shear, the floor ends have not reached the yielding stress level; this shows that the shear yield of the floor ends has not occurred.

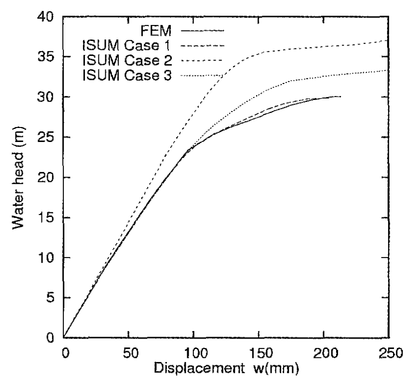


Fig. 31 Water head-central displacement relationship (model P2)

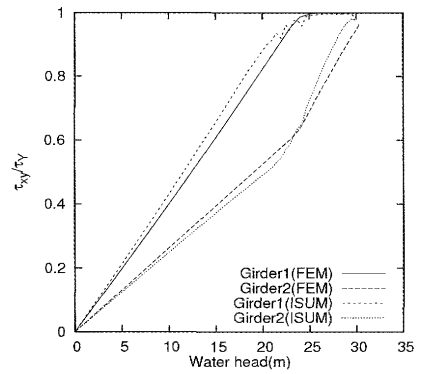


Fig. 32 Average shear stress at girder ends (model P2)

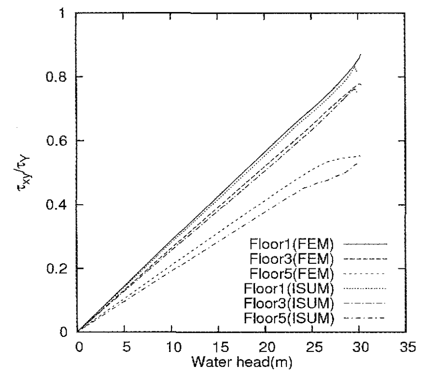


Fig. 33 Average shear stress at girder ends (model P2)

### 3.4 Collapse behavior of double bottom structure subjected to pressure load in the vertical direction

From the analysis results of models P1 and P2 shown in Section 3.3, the collapse mechanism of double bottom structure subjected to pressure load in the vertical direction are discussed. Firstly, the shear stress of the end sections of all girders and floors of Model P1 have reached the yield level at the water head of 18 m at which the structure collapses, as indicated in Fig. 25 and Fig. 26. It is also observed that the ultimate strength is decided regardless of the buckling of the flange plate from the analysis results (ISUM Case 2 and Case 3) when the out-of-plane deformation of plate elements are constrained in ISUM under conditions when buckling is prevented. From these analysis results, the shear yield of end sections of girders and floors can be considered as factors that caused the collapse of model P1. On the other hand, in case of Model P2, the girder reached the yield stress level near the water head of 30 m at which the ultimate strength is reached, as shown in Fig. 32 and Fig. 33, but the floors still have residual strength. Moreover, the results of ISUM Case 2 and Case 3 show significant differences compared to Case 1 considering buckling of the ISUM panel. From these results, the effect of buckling of bottom shell plating and buckling in in-plane bending of floors on the overall strength can be confirmed. Also, when the overall double bottom structure is viewed, the collapse of model P2 can be considered as bending collapse that occurred when the bottom shell panels and the floor panels at the central part of the double bottom buckled.

## 4. CONCLUSION

As part of the development of idealized structural unit method that enables collapse analysis of large scale structures such as hull structure by enhancing calculation efficiency, the objectives of the present research is to develop new ISUM element and to use this to realize collapse analysis of double bottom structures with high accuracy.

In Section 2, research related to ISUM element used for deflection shape function expressing buckling in in-plane bending has been carried out as part of the development of ISUM elements for expressing girder structure. The main findings of the present research are as below.

(1) When a rectangular plate is subjected to pure in-plane bending moment, mainly one half-wave and two half-wave deflection modes in the direction of the edged subjected to the moment develop. These two modes form typical buckling mode under in-plane bending in which deflection develops, biased on the compression side in bending of the structure.

(2) A basic equation expressed by general notation has been proposed to consider combining arbitrary deflection components.

(3) By comparing calculated results using the newly developed ISUM element with the calculated results by non-linear FEM, it has been confirmed that the balance of analysis accuracy and calculation costs becomes satisfactory if a deflection function with deflection components consisting of superimposition from one half-waves to four half-waves is used as a deflection shape function. However, the issue of overestimation in decreasing stress after ultimate strength remains, similar to the case of rectangular plate ISUM element subjected to in-plane compressive loads in the case of thin plates.

In section 3, the ISUM element developed in Section 2 is used in a girder structure, and collapse analysis has been performed on a double bottom structure subjected to pressure load in the vertical direction. Studies have been carried out to compare the calculated results of the same model by non-linear FEM analysis and validate the analysis accuracy at the same time. The collapse behavior of double bottom structure has been also studied based on the analysis results. The findings of the studies are as given below.

(1) Collapse analysis of one-fourth region model of a double bottom structure that required about six hours using non-linear FEM can be carried out in about 10 minutes using ISUM, thereby validating its high calculation efficiency.

(2) Collapse analysis of double bottom structure by ISUM has been performed for cases in which buckling in in-plane bending of girder web is considered/not considered. The accuracy of the solution for the case considering buckling in in-plane bending is enhanced significantly. This indicated that the ISUM element representing buckling in in-plane bending developed in Section 2 functioned correctly.

(3) The results of collapse analysis of the double bottom structure for two cases by ISUM assuming Panamax size bulk carrier are found to agree very well with the analysis results of non-linear FEM after comparison of deformation diagrams, water head-central deflection relationships, and stress distributions. The ultimate strength of the double bottom structure is estimated with good accuracy.

(4) Two kinds of collapse behaviour of double bottom structure have been observed: collapse due to shear yield of girder end sections, and bending collapse due to bending loads on girder and compression/tension load in the flange area.

A further direction of this study will be to perform collapse analysis for double bottom structures subjected to pressure load and longitudinal thrust, assuming vertical bending moment acting on the hull, simultaneously. Valuable findings on collapse behavior of double bottom structure may be obtained by studying the collapse behavior under combined loads close to the actual load condition of double bottom structures. For this, ISUM element that can represent with high accuracy the buckling collapse behavior under large compressive thrust loads and bending loads needs to be developed.

For realization of collapse analysis of ship's hold structure or the entire hull, which is the final objective of ISUM, it is necessary to develop tools that can easily generate models and indicate analysis results, in addition to the development of ISUM element with new functions required for modeling.

## ACKNOWLEDGEMENT

The authors gratefully acknowledge the guidance of Professor Tetsuya Yao of Osaka University and Professor Masahiko Fujikubo of Hiroshima University in this research. The authors are deeply indebted to both professors for their valuable guidance.

## REFERENCES

(1) Common Structural Rules for Bulk Carriers, Part CSR-B of the Rules for the Survey and Construction of Steel Ships (2006), ClassNK.

(2) Common Structural Rules for Tankers, Part CSR-T of the Rules for the Survey and Construction of Steel Ships (2006), ClassNK.

(3) Yukio Ueda, Rashed S.M.H., Katayama: Ultimate strength analysis of double bottom structures by idealized structural unit method, Journal of the Society of Naval Architecture of Japan, No. 138, pp. 322-329

(4) Yukio Ueda, S.M.H. Rashed, J.K. Paik; Development of idealized structural elements of rectangular plates and stiffener plates (Report No. 1), Journal of the Society of Naval Architecture of Japan, No. 156 (1984), pp. 366-377.

(5) Ueda. Y, Rashed, SMH and Nasser, Y:A.: An Improved ISUM Rectangular Plate Element Taking Account of Post-Ultimate Strength Behavior, Marine Structures, Vol.6 (1993), pp.139-172.

(6) Yukio Ueda, Koji Masaoka: Elastoplastic analysis method for thin plate structures using eigenfunctions – first report - rectangular plate elements receiving compressive and shear loads, Journal of the Society of Naval Architecture of Japan, No. 174 (1993) pp. 439-445.

(7) Koji Masaoka, Yukio Ueda: Elastoplastic analysis method for thin plate structures using eigenfunctions – second report – rectangular plate elements considering initial imperfections, Journal of the Society of Naval Architecture of Japan, No. 178 (1995), pp. 463-470.

(8) Fujikubo, M, Kaeding, P and Yao, T : ISUM Rectangular Plate Element with New Shape Functions(1st Report) – Longitudinal and Transverse Thrust., Journal of the Society of Naval

Architecture of Japan, No. 187 (2000), pp.209-219.
(9) Fujikubo, M, Kaeding, P and Yao, T : ISUM Rectangular Plate Element with New Shape Function s(2nd Report) -Stiffened Plates under Biaxial Thrust, Journal of the Society of Naval Architecture of Japan, No. 188 (2000), pp.479-487.
(10) Fujikubo, M and Kaeding, P : New Simplified Approach to Collapse Analysis of Stiffened Plates, Marine Structures, Vol. 15(2002), pp.251-283.
(11) Kaeding, P and Fujikubo, M ; Idealized Structural Unit Method for Collapse Analysis of Stiffened Plate Structures, Ship Technology Research, Vol. 50(2003), pp.23-33.
(12) Fujikubo, M,, Yanagihara, D, Setoyama, Y and Olaru, D.V.: ISUM Approach for Collapse Analysis of Double-Bottom Structures in Ships, Int. J. Offshore and Polar Eng, Vol.13(2003), pp.224-231.